

CHAPTER VI

MELT RHEOLOGY AND EXTRUDATE SWELL OF ORGANOBENTONITE-FILLED POLYPROPYLENE NANOCOMPOSITES

6.1 Abstract

Melt rheological properties and extrudate swell of organobentonite-filled polypropylene nanocomposites were studied by using a capillary rheometer in a shear rate range of 50-8000 s⁻¹ and a temperature range of 190-210°C. The nanocomposites exhibited shear-thinning behavior and the viscosity was well-described by the power law in this shear rate region. The addition of organobentonite enhanced the pseudoplasticity, i.e. increased the shear thinning behavior. With increasing organobentonite concentration, the shear stress/viscosity increased, while the power law index (n) decreased, and this effect is more significant at higher filler concentrations (>3 wt%). The dependence of shear viscosity on temperature obeyed the Arrhenius-Eyring expression, and the activation energy (E_a) decreased with increasing shear rate. Extrudate swell is a non-linear function of shear rate, while it is a linear function of shear stress or temperature. With increasing organobentonite concentration (>3 wt%), the extrudate swell clearly decreased, which is attributed to the limitation of the elastic recovery of the polymer chains by oriented silicate layers.

(Key-words: organobentonite; melt rheology; extrudate swell; nanocomposite; polypropylene)

6.2 Introduction

Polymer/layered silicate nanocomposites (PLS) have attracted substantial attention because of their superior physical and mechanical properties (including enhanced modulus, increased thermal stability, decreased flammability and gas permeability, increased biodegradability of biodegradable polymers) compared with virgin polymers or conventional composites (Usuki, 1997; Gilman, 1999; Yano, 1999; Sinha,2002). PLS nanocomposites can be synthesized either by in situ

polymerization of monomers (Krishnamoorti *et al.* 1996 and 1997) or by mixing silicates and polymer in solution (Ren, 2000 and Wu, 1993). For most polymers, including polyolefins, the direct melt-mixing method offers the most convenient and cost-effective means of preparing nanocomposites (Fornes, 2001; Galgali, 2001; Solomon, 2001). There are two idealized types of microstructure in PLS nanocomposites, namely, intercalated and exfoliated (or delaminated). Intercalated nanocomposites are formed when polymer chains reside between the host silicate layers with more or less fixed interlayer distances. Intercalation results in a well-ordered multilayered structure, and typically does not occur in melt-mixed materials. Exfoliated nanocomposites are formed when silicate layers are delaminated and dispersed in the polymer matrix. The exfoliated state is especially effective in improving reinforcement and other performance properties. Intermediate states are also available; for example a sample could consist of some exfoliated platelets and other platelets that exist as tactoids, i.e. layered structures with a small number of layers.

Rheological studies of PLS nanocomposites have been of interest recently because such studies offer a way to characterize the state of dispersion of layered silicate, and also provide useful guidelines for optimum processing conditions. Krishnamoorti *et al.* (1996, 1997, 2000) conducted small-strain amplitude oscillatory shear experiments of two series of end-tethered exfoliated nanocomposites based on poly(ϵ -caprolactone), nylon 6, and one series of intercalated nanocomposites based on a disordered diblock copolymer of polystyrene and polyisoprene (PSPI). The storage (G') and loss moduli (G'') of these nanocomposites increased monotonically with the silicate loading at all frequencies. At low frequency, nanocomposites containing high silicate loading exhibited a pseudo-solid-like response (i.e. G' exceeded G'' and G' was nearly independent of frequency). This pseudo-solid-like behavior at long times was attributed to randomly oriented stacks of silicate layers that formed a percolated three-dimensional network. Other researchers have found similar low frequency behavior (Fornes, 2001; Galgali, 2001; Solomon, 2001; Li, 2003; Treece, 2007; Gu, 2001). Fornes *et al.* (2001) performed oscillatory shear experiments over a wide range of frequencies using nylon 6/clay nanocomposites

with different molecular weights. High molecular weight-based nanocomposites exhibited strong non-Newtonian behavior (i.e. complex viscosity increased with decreasing frequency and the terminal zone slope was small) while the nanocomposites with low molecular weight displayed weaker Newtonian behavior (i.e. the complex viscosity was constant at frequencies less than 5 rad/s and terminal zone slope was larger). This difference was attributed to the differences in extent of exfoliation, i.e. larger extent of exfoliation led to more solid-like behavior. Using oscillatory shear experiments, Li *et al.* (2003) reported that the percolation threshold for PPCNs structure was observed with clay loadings near 3 wt% while Salomon *et al.* (2001) found a percolation threshold around 2 wt%.

Other types of rheological studies have been performed on PPCNs. The significance of compatibilizer (PP-g-MA) on the rheological behavior of PPCNs was studied by Galgali *et al.* (2001). The zero-shear viscosity (η_0) of compatibilized nanocomposites was three-orders of magnitude higher than that of the matrix and uncompatibilized nanocomposites indicating that the presence of PP-g-MA enhanced the exfoliated structure, and η_0 also decreased with annealing time. Salomon *et al.* (2001) performed non-linear reversing shear flow experiments (shear rate = 0.1 s^{-1} , 300 s, 4.8 wt% clay) in order to study the transient structural evolution during shear and the disorientation kinetics of flow-aligned silicate domains during the annealing period between deformations. The magnitude of stress overshoot was strongly dependent on the rest time. The transient stress in start-up of shear scaled with strain over a wide range ($0.005\text{-}1 \text{ s}^{-1}$) of strain rates. The authors concluded this non-linear rheology was consistent with an anisometric, non-Brownian structure, which was later confirmed by other studies (Li, 2003 and Treece, 2007). Additionally, the maximum of stress overshoots appeared at the strain of 10⁰% (Li *et al.* 2003) consistent with the strain where the deviation from linear viscoelastic behavior started. In other words, the network structure was sensitive to the strain, and could be regarded as elastic to deformations less than 10⁰%. Gu *et al.* (2004) showed that at lower frequencies, the steady shear viscosities of PPCNs increased with org-MMT content. However, the PPCN melts showed a greater shear-thinning tendency than pure PP melt because of the preferential orientation of the MMT layers. They

concluded that PPCNs had a higher moduli but better processibility compared with pure PP.

Die swell, also called extrudate swell or the Barus effect, is an important phenomenon regarding the shape/size and quality of the end products. When molten polymer flows through a capillary, molecular chains become oriented due to the applied shear. As melt leaves the die, molecular chains tend to recoil in the flow direction and grow in the normal direction, leading to extrudate swell. From the view point of macrorheology, the extrudate swell is a parameter related to the melt elasticity and occurs as a result of the recovery of the elastic deformation imposed in the capillary. Elastic recovery is affected by many factors, such as the applied shear rate/stress, temperature, L/D ratio, and the presence of fillers (Liang, 2002 and Dangtungee, 2005). For PLS nanocomposites, only a few studies have investigated extrudate swell. Chen *et al.* (2005) investigated extrudate swell of high impact polystyrene nanocomposites and found that the extrudate swell decreased linearly with a rise of temperature and decreased slightly with increasing clay loading. Zhong *et al.* (2005) attributed a large reduction of extrudate swell of PS nanocomposites vs pure PS as coming from the formation percolated network structure, which led to the enhancement of viscoelastic response (i.e. G' was higher than G'' and G' leveled-off at low frequencies) in the former. Sadhu *et al.* (2005) reported a similar observation for three types of rubber-based nanocomposite (styrene butadiene rubber, acrylonitrile butadiene rubber and polybutadiene rubber); the die swell decreased with increasing clay. In addition, they studied the effect of unmodified and modified-clay on the die swell and found that the modified-clay nanocomposites exhibited a lower die swell than unmodified nanocomposites which was attributed to better dispersion/exfoliation of modified-clay in the rubber matrix.

In this work, we investigated the effects of the shear stress, testing temperature, and filler concentration on the melt rheology and extrudate swell of organobentonite-filled polypropylene nanocomposites via capillary rheometry.

6.3 Results and Discussion

6.3.1 Flow Properties

A flow curve is an important method to characterize the processing properties of polymer melt and is represented by a graph of shear stress vs. shear rate. Figure 6.1 shows logarithmic plots of the apparent shear stress versus apparent shear rate of unfilled and organobentonite-filled systems at 190°C for various organobentonite concentrations. The apparent shear stress of both unfilled and organobentonite-filled PP nanocomposites increases approximately linearly with increasing apparent shear rate with a slope less than 1, indicating that the melts for all samples obey the power law over the entire studied range of shear rate. With an increase in organobentonite concentrations, the shear stress increases, but the difference are small and tend to converge at high shear rate. The effect of organobentonite concentrations on the flow properties of the PP nanocomposites will be discussed in Section 6.3.2.

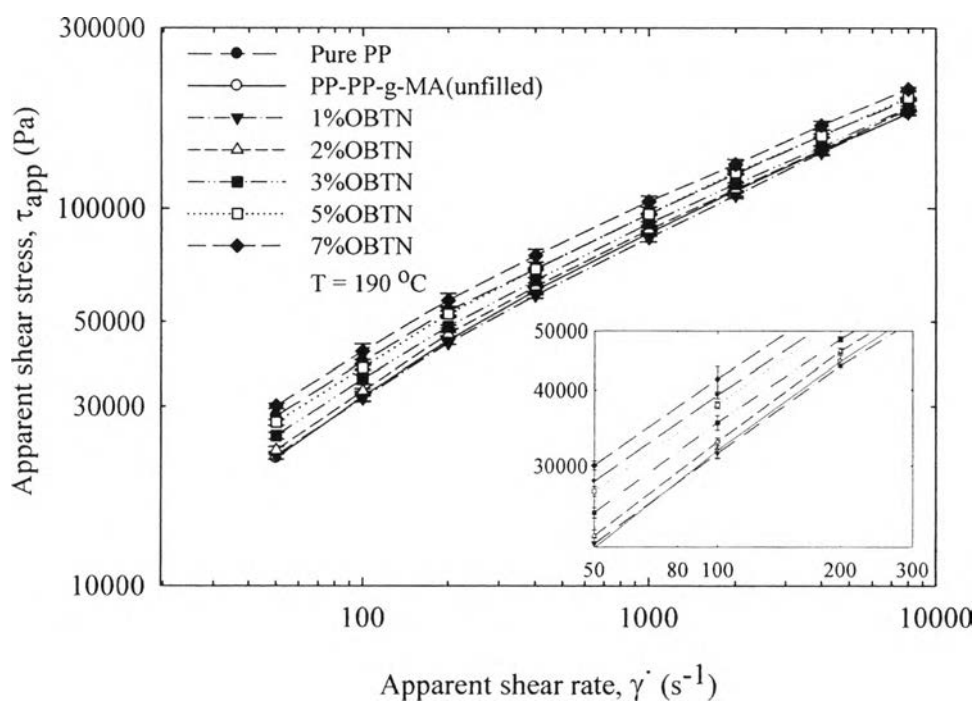


Figure 6.1 Apparent shear stress of organobentonite-filled PP nanocomposites as function of apparent shear rate at varying OBTN concentrations.

Figure 6.2 illustrates the dependence of apparent shear viscosity on the apparent shear rate of both unfilled and organobentonite-filled PP nanocomposites confirming shear-thinning (i.e. pseudoplastic) behavior of these PP/organobentonite nanocomposites. Generally speaking, pseudoplastic behavior can arise in either of two ways (Bryson, 1981). In one case, asymmetric molecular chains are extensively entangled and/or randomly oriented at rest. Under shear, molecular chains become oriented, and the numbers of entanglements are reduced; as a result of which the viscosity decreases. At very high shear rate, the orientation may be complete, and near-Newtonian behavior may be observed. In the other case, highly solvated molecular chains may be present. With increasing shear rate, the solvated layers may be sheared away, resulting in decreased viscosity (Li *et al.* 1999).

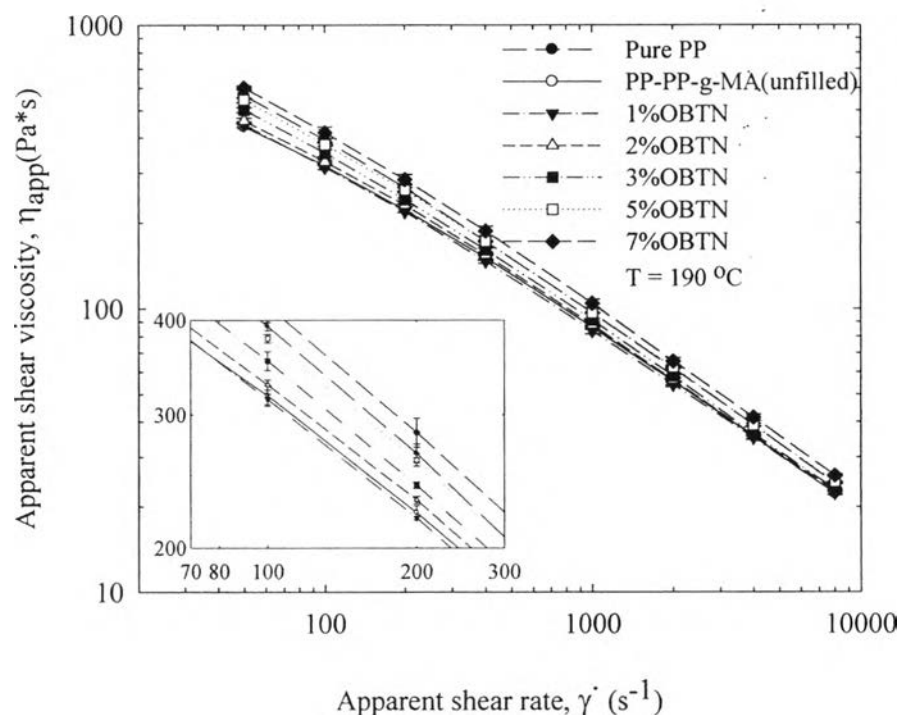


Figure 6.2 Apparent shear viscosity of organobentonite-filled PP nanocomposites as a function of apparent shear rate at varying OBTN concentrations.

6.3.2 Effect of Filler Concentrations

Figure 6.1 and 6.2 show that organobentonite-filled PP nanocomposites follow the power law relation; Figure 6.3 replots the data in Figure 6. 2 to illustrate more clearly the influence of organobentonite concentrations on the apparent shear viscosity. The shear viscosity of nanocomposites increases as filler concentration is increased due to the inhibition of the polymer chain motion by the filler particles (Liang, 2002). Interestingly, at low shear rate the addition of small amounts of clay results in a significant enhancement in the apparent shear viscosity. At high shear rate, the shear viscosities for the nanocomposites are comparable with or even lower than that of the pure PP. In other words, the viscosities for the nanocomposites tend to converge at higher shear rates due to the lesser pseudoplasticity of clay-filled systems, i.e. the power law exponent n is lower. This result is quite consistent with other PP-based nanocomposites (Gu *et al.* 2004) as well as HIPS-based nanocomposites (Chen *et al.* 2005), rubber-based nanocomposites (Bryson, 1981) and nylon 6-based nanocomposites (Ren and Krishnamoorti, 2003). The fact that differences in viscosity with higher clay concentration are lower at higher shear rates could be due to the more oriented clay layers or anisotropic tactoids, or perhaps even the percolation network structure is becoming more oriented along the flow direction.

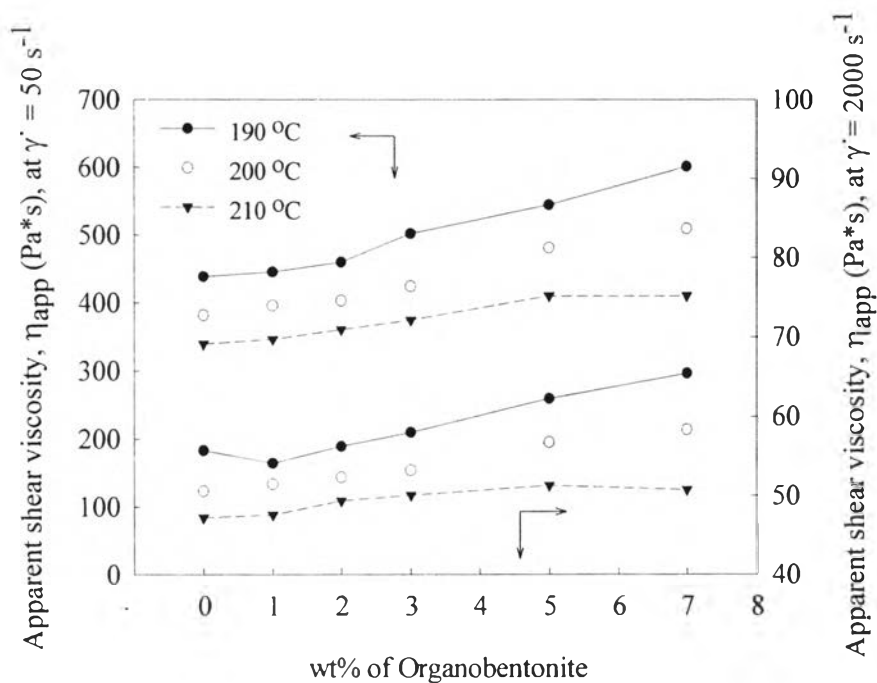


Figure 6.3 Apparent shear viscosity as a function of organobentonite concentrations at two constant shear rates (50 and 2000 s^{-1}) and various temperatures.

6.3.3 Effect of Temperature

In a polymer melt, the viscosity decreases with increasing temperature due to greater free space available for molecular chain motion at higher temperature (Saini *et al.* 1986). Figure 6.4 shows that increasing temperature decreases the apparent shear viscosity of 5 wt% organobentonite-filled PP nanocomposites. The temperature sensitivity is more pronounced at lower shear rates due to the fact that high shear rates lead to a decrease of the entanglement density of the polymer chains and this decrease is likely to occur independent of the diffusive motion of the chains (Li *et al.* 1999). The temperature dependence of shear viscosity of these PP/organobentonite nanocomposites was fitted using the following Arrhenius-Frenkel Eyring equation:

$$\eta_{app} = A_0 \exp\left(\frac{E_a}{RT}\right) \quad (5)$$

where η_{app} is the apparent shear viscosity at a particular shear rate, A_0 is a constant, and R , T , and E_a are taken to be the universal gas constant, the absolute temperature, and the activation energy of melt flow respectively. E_a values, summarized in

Table 6.1, were calculated from the slope obtained by the linear regression of plot between $\ln \eta_{app}$ vs. $1/T$ at various shear rates (Figure 6.5). E_a gradually decreases with increasing shear rate, i.e. the viscosity changes less with increasing temperature, which is attributed to the fact that shearing reduces entanglements and hence results in a decrease of interaction between chain segments (Li *et al.* 1999). E_a values of unfilled and 1-3 wt% organobentonite-filled systems are nearly the same and then become higher with a further increase in filler concentrations (>3 wt% OBTN), especially at lower shear rates. In other words, the highly-filled system is more temperature sensitive than the lower-filled or unfilled systems presumably due to the limitation of molecular chain motion by aggregated filler particles; and hence, enhancement of the activation energy. This result is consistent with previous work from linear rheological measurement as reported by Gu *et al.* (2004). They suggested that the higher flow activation energy causes a larger energetic barrier for segmented motions in the confined space and thus causes an increase of G' , G'' , and η^* . The increasing flow activation energy of PP-clay nanocomposites was also strengthened because of the strong hydrogen bonding between the polar functional group of PP-g-MA and the oxygen group of montmorillonite. However, the work by Gu and the work reported here is not consistent with that reported by Galgali *et al.* (2001). These authors found that the activation energy of PP nanocomposite with 6 wt% clay was nearly the same as that of PP/PP-g-MA or of pure PP systems.

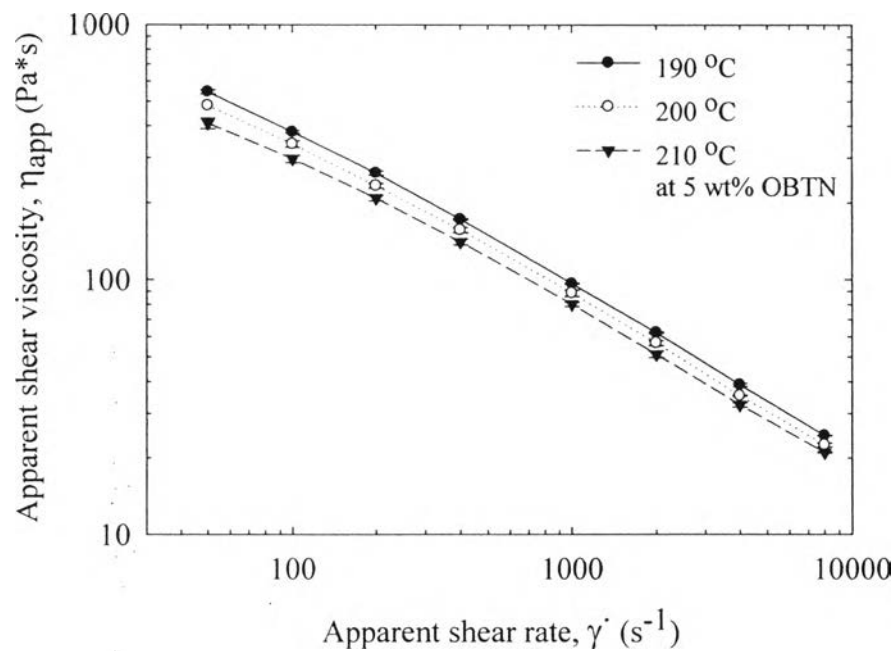


Figure 6.4 Apparent shear viscosity for 5 wt% of organobentonite-filled PP nanocomposites as a function of shear rates at various temperatures.

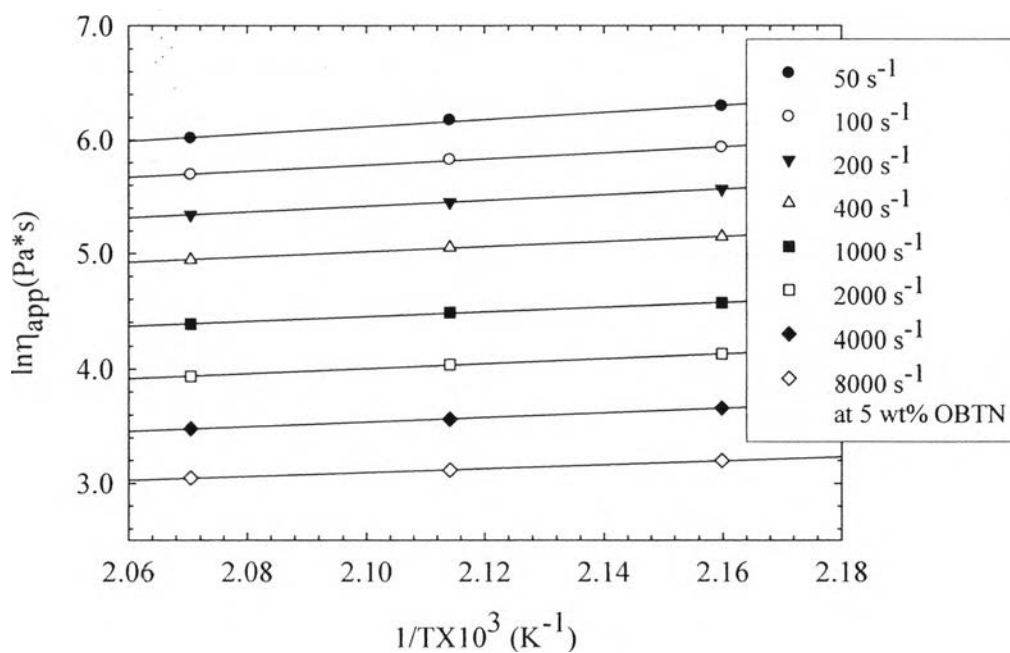


Figure 6.5 Apparent shear viscosity of 5 wt% of organobentonite-filled PP nanocomposites as a function of reciprocal temperatures ($1/T$) at various shear rates.

6.3.4 Power Law Exponent (n)

As mentioned previously, Figure 6.1 shows a linear relationship between apparent shear stress and shear rate in a bi-logarithmic coordination system in the studied shear rate range, indicating that the melt shear flow of unfilled and organobentonite-filled systems obeys the power law relationship:

$$\tau_{app} = K \dot{\gamma}_{app}^n \quad (6)$$

K is the melt viscosity coefficient, with a high value being an indication of a more viscous material; and n is the power law index, with a lower value an indication of a more pseudoplastic material. K and n values obtained by linear regression are listed in Table 6.2. With a rise in temperature, the values of n for both systems increase monotonously, i.e. the materials become less pseudoplastic. Contrarily, n decreases slightly with increasing organobentonite concentrations, i.e. the material becomes more pseudoplastic. This observation is qualitatively the same but quantitatively different from the result obtained by Gu *et al.* (2004) who reported that the addition of clay leads a much larger decrease of n (value of n for PP, PPCN5, and PPCN7 were 0.7679, 0.5388, and 0.5294, respectively).

Table 6.1 Activation energy (E_a) for viscous flow of organobentonite-filled PP nanocomposites at various shear rates

Compositions (PP/PP-g-MA/%Organoclay)	E_a (kJ/mol)							
	50 s ⁻¹	100 s ⁻¹	200 s ⁻¹	400 s ⁻¹	1000 s ⁻¹	2000 s ⁻¹	4000 s ⁻¹	8000 s ⁻¹
100/0/0 (Pure PP)	23.79	21.62	19.12	15.02	13.16	12.24	13.36	12.34
85/15/0 (PP-PP-g-MA) (unfilled)	23.79	20.77	18.75	17.96	14.92	15.39	15.04	11.61
84/15/1 wt% OBTN	23.35	19.67	15.45	13.19	11.72	11.96	13.58	12.77
83/15/2 wt% OBTN	22.56	17.58	17.95	14.97	13.29	12.18	11.52	11.49
82/15/3 wt% OBTN	27.23	23.12	19.60	16.77	14.82	13.73	13.11	11.90
80/15/5 wt% OBTN	26.31	22.47	21.05	18.98	17.15	18.00	16.86	14.32
78/15/7 wt% OBTN	35.50	32.70	30.47	27.92	25.58	23.60	24.84	23.97

Table 6.2 Power law exponent (n) and melt viscosity coefficient (K) of organobentonite-filled PP nanocomposites at various temperatures

Compositions (PP/PP-g-MA/%Organoclay)	190°C		200°C		210°C	
	K (kPa)	n	K (kPa)	n	K (kPa)	n
100/0/0 (Pure PP)	3.844	0.3765	3.726	0.3987	3.698	0.4006
85/15/0 (PP-PP-g-MA) (unfilled)	3.688	0.4085	3.609	0.4197	3.546	0.4306
84/15/1 wt% OBTN	3.688	0.4064	3.634	0.4146	3.560	0.4266
83/15/2 wt% OBTN	3.717	0.4021	3.647	0.4130	3.584	0.4241
82/15/3 wt% OBTN	3.774	0.3885	3.672	0.4088	3.606	0.4192
80/15/5 wt% OBTN	3.812	0.3856	3.750	0.3922	3.661	0.4070
78/15/7 wt% OBTN	3.872	0.3758	3.777	0.3878	3.671	0.4007

6.3.5 Extrudate Swell

6.3.5.1 Effect of Shear Rate and Filler Concentration on Extrudate Swell

Extrudate swell varies by shear rate, temperature, die length, and filler type (Dangtungee, 2005; Liang, 2002; Chen, 2005). Figure 6.6 illustrates the dependence of extrudate swell on apparent shear rate and filler concentrations at 190°C. Extrudate swell of all materials increase with an increase in apparent shear rate in a non-linear relationship. At the lower apparent shear rate range (50-200 s⁻¹), extrudate swell increases gradually, and increases more sharply at higher apparent shear rates (400-8000 s⁻¹). At higher shear rates, the recoverable elastic energy stored in the polymer melt flow increases, which results in an increase of extrudate swell.

Extrudate swell occurs due to the recovery of elastic deformation imposed in the capillary. The presence of filler can increase energy dissipation of the system by movement of the filler, which can be easier than that of the polymeric chains for the given shear rate. Hence the elasticity recovery, and consequently the extrudate swell of a filled polymer, is less than for the unfilled material. Figure 6.6 clearly shows that the extrudate swell of the organobentonite-filled system is lower than that of the unfilled PP. With increasing organobentonite concentrations, extrudate swell drops markedly, especially in the high shear rate region. A similar trend was observed in the case of uncoated and stearic acid-coated CaCO₃-highly filled PP composites (Dangtungee *et al.* 2005), Org-MMT-filled HIPS, PS, and rubber nanocomposites (Chen, 2005; Zhong, 2005; Sadhu, 2005). Chen *et al.* (2005) rationalized this effect in that the oriented layered silicates limit the elastic recovery of the confined molecular chains in a plane vertical to the extrusion direction after leaving the capillary die, resulting in lower extrudate swell.

Scanning electron micrographs of the extrudates are shown in Figure 6.7(a) and 6.7(b), respectively. Figure 6.7(a) shows that the diameter of these extrudates increases with increasing shear rate, while Figure 6.7(b) shows that the presence of organobentonite particles can reduce the severity of the extrudate swell. The extrudates of the organobentonite-filled system exhibit more surface roughness than those of unfilled PP systems possibly due to the fact that the elastic response was larger in the latter. However, Sadhu *et al.* (2005) observed the different result for

the case of rubber-based nanocomposites. The surface smoothness was increased on incorporation of the modified clay.

6.3.5.2 *Effect of Temperature on Extrudate Swell*

Figure 6.8 shows the relationship between extrudate swell and testing temperatures for 5 wt% organobentonite-filled PP nanocomposites at various apparent shear rates. Extrudate swell at various shear rates decreases linearly with a rise of temperature and the slope moves upward with increasing apparent shear rate. The correlation between extrudate swell (B) and the temperature (T) can be represented as follows (Liang and Ness, 1998):

$$B = \alpha_1 - \beta_1 T \quad (7)$$

where α_1 and β_1 are the coefficients related to the material properties. The result of a linear fit to this expression is summarized in Table 6.3. At lower shear rates (50-2000 s^{-1}), the sensitivity of B on the test temperature is less significant, but the sensitivity of B on temperature is more obvious (i.e. β_1 decreases sharply) at higher shear rates (4000-8000 s^{-1}). This phenomenon is possibly due to the fact that with a rise of temperature, the motion of the molecular chains is quickened and the relaxation process of the melt is shortened, leading to a reduction of the elastic recovery of the melt when it emerges from the die. Hence, the extrudate swell of the nanocomposite is considerably reduced (Laing, 2002). Furthermore, the ability of the melt to recover to its original structure is less at higher temperature because the viscous response is much greater than the elastic response, and consequently the extent of the swell of these extrudates is also less.

6.3.5.3 *Effect of Shear Stress and Filler Concentrations on Extrudate Swell*

Figure 6.9 illustrates the relationship between the extrudate swell and apparent shear stress for both unfilled and various organobentonite-filled systems for a test temperature of 190°C. These plots show that the extrudate swell increases linearly with increasing apparent shear stress for all melts. This observation is similar to the results obtained by Liang (2002 and 2004) in the case of glass bead-

filled iPP, CaCO₃-filled natural rubber, and carbon black-filled natural rubber. The linearity between the extrudate swell (B) and the apparent shear stress (τ_{app}) can be expressed as follow (Li *et al.* 1999):

$$B = B_0 + B_1 \tau_{app}, \quad (7)$$

when B_0 and B_1 are constants related to the melt elasticity of the materials. Values of B_0 and B_1 are summarized in Table 6.4.

As stated previously, increasing the apparent shear stress causes the shear rate and the shear deformational energy stored in the molecular chains to also increase (with the temperature fixed), leading to a corresponding increase in the extrudate swell. B_1 decreases slightly when the organobentonite concentration increases to 3 wt%. With further increasing organobentonite concentrations (5-7 wt%), the slope falls sharply. As mentioned above, the decrease in B_1 values, or decrease in the extrudate swell, with increasing organobentonite concentration occurs because the presence of filler particles limit motion of the matrix chains; thus the elastic recovery of the shear deformation will be reduced. Possibly, higher shear stress may cause some agglomerates to break apart, leading to the better filler dispersion observation, thus being able to keep the polymer matrix from swelling (Samsudin *et al.* 2006).

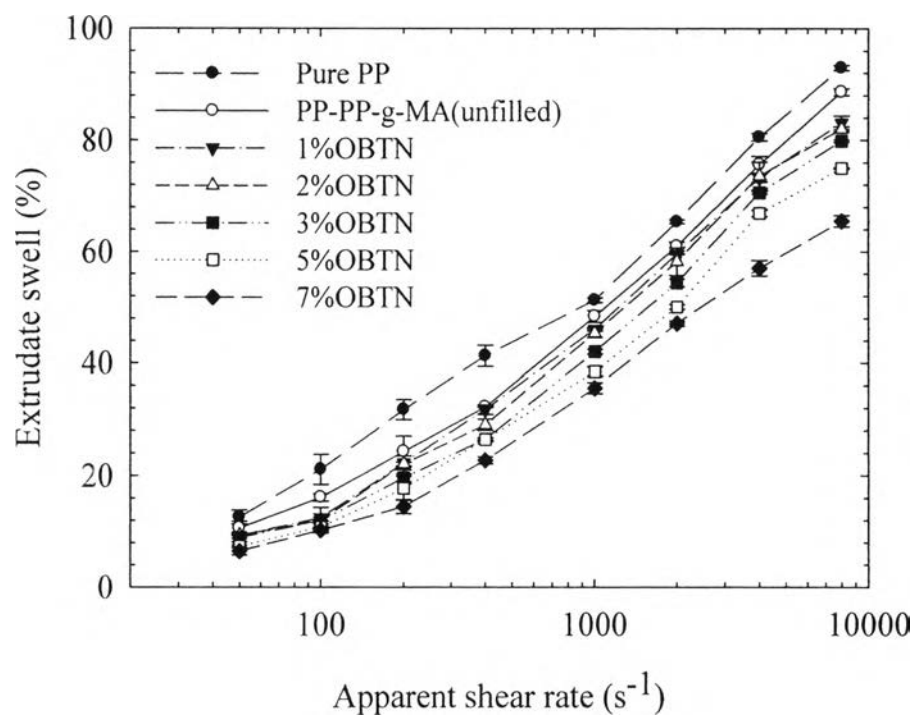
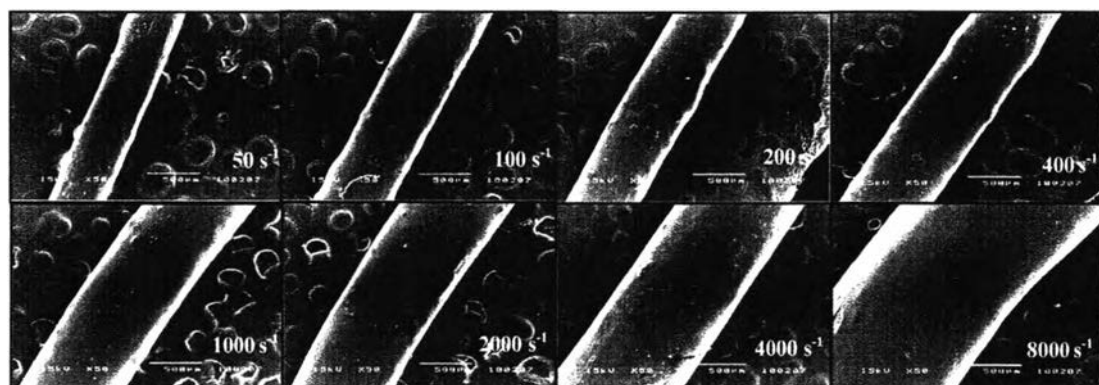
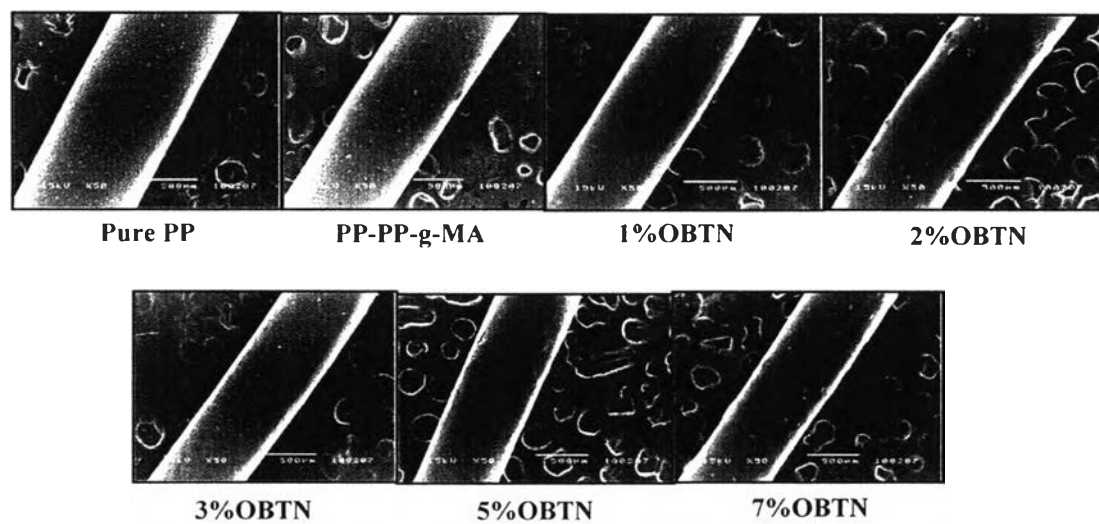


Figure 6.6 Extrudate swell (%) of unfilled and organobentonite-filled PP nanocomposites as a function of apparent shear rates (190°C).



(a)



(b)

Figure 6.7 SEM micrographs of the extrudates obtained at 210°C: (a) effect of the apparent shear rates (at 5 wt% OBTN filled); and, (b) effect of OBTN concentrations (at a fixed $\gamma_{app} = 400\text{s}^{-1}$).

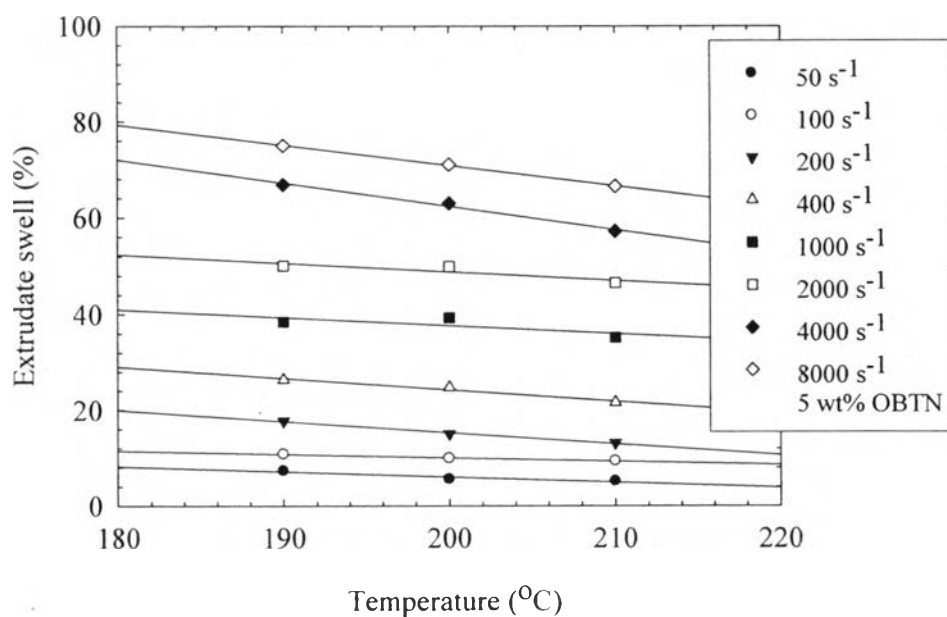


Figure 6.8 Extrudate swell for 5 wt% organobentonite-filled PP nanocomposite as a function of temperature at various apparent shear rates.

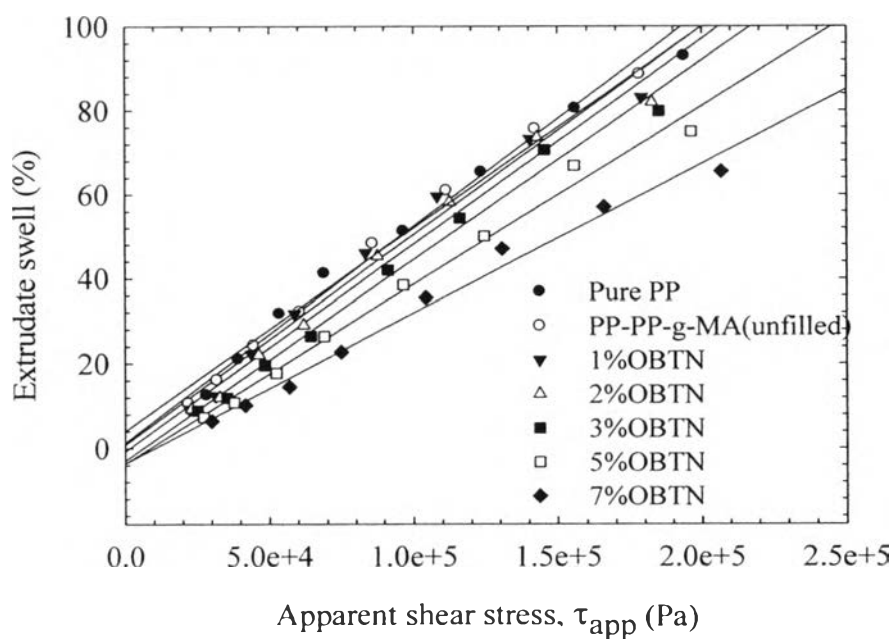


Figure 6.9 Extrudate swell (%) of organobentonite-filled PP nanocomposites as a function of apparent shear stress (at 190°C).

Table 6.3 The values of α_1 and β_1 for 5 wt% organobentonite-filled PP nanocomposites at various shear rates

Apparent shear rate (s^{-1})	Effect of T on B (at 5 wt% OBTN)		
	α_1	β_1	R
50	27.75	-0.1086	0.885485
100	24.45	-0.0721	0.981683
200	61.77	-0.2324	0.990906
400	72.42	-0.2409	0.965745
1000	70.75	-0.1654	0.568822
2000	84.17	-0.1767	0.781800
4000	158.8	-0.4822	0.987586
8000	155.5	-0.4232	0.998378

Table 6.4 The values of melt elasticity constants, B_0 and B_1 for unfilled and organobentonite-filled PP nanocomposites

Compositions (PP/PP-g-MA/%Organoclay)	B_0	B_1 (Pa^{-1})	R
100/0/0 (Pure PP)	4.0560	0.000480	0.986807
85/15/0 (PP-PP-g-MA)	1.3560	0.000511	0.993005
84/15/1 wt% OBTN	0.8509	0.000496	0.978700
83/15/2 wt% OBTN	-0.6980	0.000489	0.981327
82/15/3 wt% OBTN	-0.2931	0.000475	0.988485
80/15/5 wt% OBTN	-3.5910	0.000423	0.989431
78/15/7 wt% OBTN	-3.5870	0.000355	0.985745

6.4 Conclusions

Melt rheological properties and extrudate swell behavior of organobentonite-filled polypropylene nanocomposites were investigated using a capillary rheometer. The relationship between shear stress and shear rate was well described by the power law. The incorporation of an organobentonite filler enhances the pseudoplasticity of polypropylene, i.e. the material becomes more shear-thinning. With increasing filler concentration, the shear viscosity increases while the power law index (n) decreases. The dependence of shear viscosity on testing temperature was studied, and the relationship obeys the Arrhenius-Frenkel Eyring expression. The activation energy (E_a) decreases gradually with an increasing of shear rate and increases sharply with filler concentration at or above 3wt%. Extrudate swell increases non-linearly with increasing shear rate, but increases linearly with increasing shear stress and/or decreasing temperature. Lastly, with increasing organobentonite concentration ($> 3\text{wt}\%$), the extrudate swell decreases, especially at higher shear rates, which is attributed to the limitation of the elastic recovery of the confined polymer chains by highly orientated silicate layers after capillary extrusion.